PHYSICAL REVIEW D VOLUME 47, NUMBER 9 1 MAY 1993

$\chi_{c0,c2}\to\rho\rho$ decays and the ρ polarization: Massless versus constituent quarks

Mauro Anselmino
Dipartimento di Fisica Teorica, Università di Torino and Istituto Nazionale di Fisica Nucleare, Sezione di Torino, via Pietro Giuria 1, I-10125 Torino, Italy

Francesco Murgia
Istituto Nazionale di Fisica Nucleare, Sezione di Cagliari, via Ada Negri 18, I-09127 Cagliari, Italy

(Received 22 October 1992)

We compute the helicity density matrix of vector mesons produced in the decays $\chi_{c0,c2}\to M_1M_2$, in the framework of perturbative QCD, allowing for mass corrections. Both the case in which the light quarks inside the final mesons are treated as massless current quarks and the case in which they are seen as constituent massive ones are considered. Explicit results are given for the helicity density matrix of ρ mesons, $\rho(\rho)$, showing significant differences between the two cases; the measurement of $\rho(\rho)$ should then allow a precise evaluation of these mass effects.

PACS number(s): 13.25.+m, 12.38.Bx, 13.88.+e, 14.40.Gx

I. INTRODUCTION

Many two-body charmonium decays [1–7] and some of their peculiarities [8–10] have been discussed in the literature. The modest Q^2 values involved in these processes ($Q^2 \lesssim 10$ GeV^2) are such that higher-order and nonperturbative corrections to the asymptotic QCD scheme [11–14] might still be important and, in some cases, give the dominant contributions. Indeed, comparisons of the theoretical predictions with the available data show both excellent agreements and bad failures [15]. All failures can be traced down to the helicity-conserving coupling of gluons with massless quarks and the subsequent helicity conservation and selection rule [1], which forbids many charmonium decays [2]; several of these decays, however, have been observed [9,10,15].

Among the various attempts to explain these "forbidden" decays, two-quark correlations [16–18], mass effects [9,10], higher-order Fock states [14,19], and gluonic contributions [8,20] have been considered. Obviously, two-quark correlations, or diquarks, can only be helpful for decays into final baryons and gluonic components seem to be present only in J/ψ [8] and η_c [20]. By mass effects we mean assigning the final quarks their constituent rather than their (tiny) current masses; that is, in the small Q^2 region of charmonium decays, the constituent quarks, i.e., the current quarks surrounded by their clouds of $q\bar{q}$ pairs and gluons, still act as single Dirac particles [21]. These mass corrections somehow also include, nonperturbatively, higher-order Fock state contributions.

In this paper we consider some nonforbidden decays, namely, $\chi_{c0,c2}\to M_1M_2$ (where M denotes a vector meson), and compute, both in perturbative massless QCD and in the constituent quark model (mass effects), the helicity density matrix of one of the final mesons, $\rho(M)$. Such a quantity, being a ratio of squared amplitudes, shows much less dependence on the parameters of the model [value of the charmonium wave functions at the origin, final hadron distribution amplitudes, value of $\alpha_s(Q^2)$] than the decay width, and proves a better way of evaluating the significance of the mass effects. Measurements of $\rho(M)$ should be available in the near future.

The paper is organized as follows. In Sec. II we recall the computation of the helicity amplitudes for the decays $\chi_{c0,c2}\to M_1M_2$, and give their explicit expressions $A_{\lambda_1\lambda_2;M}$. In Sec. III we discuss the formalism for computing the final meson helicity density matrix $\rho(M)$ and the way of measuring its matrix elements, by studying the angular distribution of the meson decay. Explicit expressions for $\rho_{\lambda\lambda'}(M)$, in case of χ_{c0} and χ_{c2} decays, are given in Sec. IV and numerical results, mainly for ρ mesons, are presented in Sec. V. Comments and conclusions are given in Sec. VI.

II. HELICITY AMPLITUDES FOR THE DECAY $\chi_{c0,c2}\to M_1M_2$

In perturbative QCD [11–14,22] the charmonium decay amplitudes are given by the convolution of the elementary constituent interaction amplitudes, computed according to the Feynman diagrams shown, for the case of interest here, in Fig. 1, with the charmonium and final particle wave functions. Details of such a procedure can be found in Refs. [10,16,23], to which we refer.

The decay amplitudes for $\chi_{c0,c2}\to M_1M_2$ processes can be found, for massless quarks, in Ref. [14] and, for massive quarks, limitedly to the case of longitudinally polarized vector mesons, in Refs. [10,23]. We consider here the most general case of both longitudinally and transversely polarized vector mesons with massive quarks; our results agree with the existing ones in all cases when a comparison is possible [10,14,23].

In the case of the χ_{c0} state ($L=S=1$, $J=0$) one finds, for the decay into two vector mesons M_1 and M_2 with helicity λ_1 and λ_2, the following nonzero decay amplitudes $A^{\chi_{c0}}_{\lambda_1\lambda_2}$:

$$A^{\chi_{c0}}_{1,1}=i\frac{2^{13}}{9\sqrt{3}}\pi^3\alpha_s^2\epsilon^2\frac{|R'(0)|}{M_\chi^4}f_T^2 I^{\chi_{c0}}_{1,1}(\epsilon) , \tag{2.1}$$

$$A^{\chi_{c0}}_{-1,-1}=A^{\chi_{c0}}_{1,1} , \tag{2.2}$$

$$A^{\chi_{c0}}_{0,0}=-i\frac{2^{12}}{9\sqrt{3}}\pi^3\alpha_s^2\frac{|R'(0)|}{M_\chi^4}f_L^2 I^{\chi_{c0}}_{0,0}(\epsilon) , \tag{2.3}$$

where

$$I^{\chi_{c0}}_{1,1}(\epsilon)=-\frac{1}{32}\int_0^1 dx\,dy\,\varphi_T(x)\varphi_T(y)\frac{1}{xy+(x-y)^2\epsilon^2}\,\frac{1}{(1-x)(1-y)+(x-y)^2\epsilon^2}\times\frac{1}{2xy-x-y+2(x-y)^2\epsilon^2}\left[1+\frac{1}{2}\frac{(x-y)^2(1-4\epsilon^2)}{2xy-x-y+2(x-y)^2\epsilon^2}\right] , \tag{2.4}$$

$$I^{\chi_{c0}}_{0,0}(\epsilon)=-\frac{1}{32}\int_0^1 dx\,dy\,\varphi_L(x)\varphi_L(y)\frac{1}{xy+(x-y)^2\epsilon^2}\,\frac{1}{(1-x)(1-y)+(x-y)^2\epsilon^2}\times\frac{1}{2xy-x-y+2(x-y)^2\epsilon^2}\left[1-\frac{1}{2}\frac{(x-y)^2(1-4\epsilon^2)}{2xy-x-y+2(x-y)^2\epsilon^2}-2\epsilon^2\left[1+\frac{1}{2}\frac{(x-y)^2(1-4\epsilon^2)}{2xy-x-y+2(x-y)^2\epsilon^2}\right]\right] . \tag{2.5}$$

In Eqs. (2.1)–(2.5) f_L and f_T denote, respectively, the decay constants for longitudinally and transversely polarized vector mesons [14]. φ_L and φ_T are the distribution amplitudes of quarks inside the final hadrons and, in general, one allows different distribution amplitudes for longitudinally polarized (φ_L) or transversely polarized (φ_T) vector mesons [14]. Here M_χ denotes the χ_{c0} mass and the quantity ϵ is defined as

$$\epsilon=m/M_\chi , \tag{2.6}$$

where m is the final hadron mass.

In deriving Eqs. (2.1)–(2.5) we have assigned the quarks in the final hadrons a mass $m_q=xm$ [10], where x is the fraction of hadron momentum carried by the quark (see Fig. 1); in the asymptotic limit, where lowest-order perturbative QCD is expected to dominate, $\epsilon\to 0$ and the only nonzero helicity amplitude is $A^{\chi_{c0}}_{0,0}$; only longitudinally polarized vector mesons can be produced in the decay of a very heavy spinless state [14].

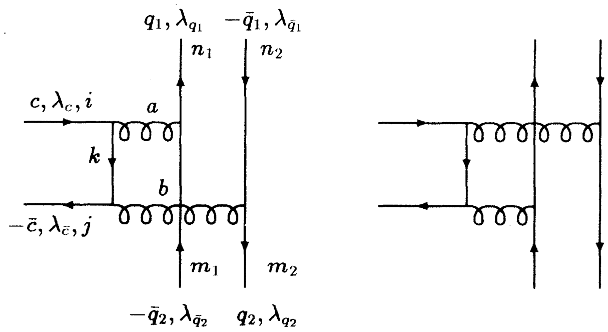

FIG. 1. Elementary Feynman diagrams contributing, to lowest order in α_s, to $\chi_{c0,c2}\to M_1M_2$ decays. In the $\chi_{c0,c2}$ center-of-mass frame, the final mesons four-momenta are $p_1^\mu=(E,\mathbf{p})$, $p_2^\mu=(E,-\mathbf{p})$, with $E=M_\chi/2$ and $\mathbf{p}=(p\sin\theta\cos\varphi,p\sin\theta\sin\varphi,p\cos\theta)$. The constituent four-momenta are $c^\mu=(E,\mathbf{k}/2)$, $\bar{c}^\mu=(E,-\mathbf{k}/2)$, with $\mathbf{k}=(k\sin\alpha\cos\beta,k\sin\alpha\sin\beta,k\cos\alpha)$, $q_1=xp_1$, $\bar{q}_1=(1-x)p_1$, $q_2=(1-y)p_2$, $\bar{q}_2=yp_2$. $a,b,i,j,k,m_{1,2},n_{1,2}$ are color indices; the λ's label helicities.

Similarly, for the $\chi_{c2}\to M_1M_2$ decay, one has

$$A^{\chi_{c2}}_{\lambda_1\lambda_2;M}=\tilde{A}_{\lambda_1\lambda_2}e^{iM\varphi}d^2_{M\lambda}(\theta),\quad \lambda=\lambda_1-\lambda_2 , \tag{2.7}$$

where θ and φ are, respectively, the polar and azimuthal decay angles of the particle M_1 (in the χ_{c2} rest frame) and M denotes the z component of the χ_{c2} spin; the "reduced" decay amplitudes $\tilde{A}_{\lambda_1\lambda_2}$ are given by

$$\tilde{A}_{1,1}=-i\frac{2^{13}\sqrt{2}}{9\sqrt{3}}\pi^3\alpha_s^2\epsilon^2\frac{|R'(0)|}{M_\chi^4}f_T^2 I^{\chi_{c2}}_{1,1}(\epsilon)=\tilde{A}_{-1,-1} , \tag{2.8}$$

$$\tilde{A}_{1,0}=-i\frac{2^{12}\sqrt{2}}{9}\pi^3\alpha_s^2\epsilon\frac{|R'(0)|}{M_\chi^4}f_T f_L I^{\chi_{c2}}_{1,0}(\epsilon)=\tilde{A}_{0,1}=\tilde{A}_{-1,0}=\tilde{A}_{0,-1} , \tag{2.9}$$

$$\tilde{A}_{1,-1}=-i\frac{2^{12}}{9}\pi^3\alpha_s^2\frac{|R'(0)|}{M_\chi^4}f_T^2 I^{\chi_{c2}}_{1,-1}(\epsilon)=\tilde{A}_{-1,1} , \tag{2.10}$$

$$\tilde{A}_{0,0}=-i\frac{2^{11}\sqrt{2}}{9\sqrt{3}}\pi^3\alpha_s^2\frac{|R'(0)|}{M_\chi^4}f_L^2 I^{\chi_{c2}}_{0,0}(\epsilon) \tag{2.11}$$

with [see Eq. (2.4)]

$$I^{\chi_{c2}}_{1,1}(\epsilon)=I^{\chi_{c0}}_{1,1}(\epsilon) \tag{2.12}$$

and

$$I^{\chi_{c2}}_{1,0}(\epsilon)=-\frac{1}{32}\int_0^1 dx\, dy\, \varphi_T(x)\varphi_L(y)\frac{1}{xy+(x-y)^2\epsilon^2}\frac{1}{(1-x)(1-y)+(x-y)^2\epsilon^2}$$
$$\times\frac{1}{2xy-x-y+2(x-y)^2\epsilon^2}\left[1+\frac{1}{2}\frac{(x-y)^2(1-4\epsilon^2)}{2xy-x-y+2(x-y)^2\epsilon^2}\right], \qquad (2.13)$$

$$I^{\chi_{c2}}_{1,-1}(\epsilon)=-\frac{1}{32}\int_0^1 dx\, dy\, \varphi_T(x)\varphi_T(y)\frac{1}{xy+(x-y)^2\epsilon^2}\frac{1}{(1-x)(1-y)+(x-y)^2\epsilon^2}\frac{1}{2xy-x-y+2(x-y)^2\epsilon^2}, \qquad (2.14)$$

$$I^{\chi_{c2}}_{0,0}=-\frac{1}{32}\int_0^1 dx\, dy\, \varphi_L(x)\varphi_L(y)\frac{1}{xy+(x-y)^2\epsilon^2}\frac{1}{(1-x)(1-y)+(x-y)^2\epsilon^2}$$
$$\times\frac{1}{2xy-x-y+2(x-y)^2\epsilon^2}\left[1+\frac{(x-y)^2(1-4\epsilon^2)}{2xy-x-y+2(x-y)^2\epsilon^2}\right.$$
$$\left.+4\epsilon^2\left[1+\frac{1}{2}\frac{(x-y)^2(1-4\epsilon^2)}{2xy-x-y+2(x-y)^2\epsilon^2}\right]\right]. \qquad (2.15)$$

In Eqs. (2.8)–(2.15) $m_q=xm$ is the final quark mass, M_χ is the χ_{c2} mass and ϵ is defined as in Eq. (2.6). Again, one recovers the usual massless perturbative QCD results [14] in the limit $\epsilon\rightarrow 0$; in such a limit only the $A^{\chi_{c2}}_{1,-1;M}$ and $A^{\chi_{c2}}_{00;M}$ amplitudes do not vanish and the final vector mesons are produced with opposite helicities, according to the helicity conservation rule [1].

III. FINAL MESON HELICITY DENSITY MATRIX

Let us now consider one of the vector mesons produced in the charmonium decay, for example, M_1. Its helicity density matrix is defined as [24]

$$\rho_{\lambda_1\lambda_1'}(M_1)=\frac{1}{N}\sum_{\lambda_2,M,M'}A_{\lambda_1\lambda_2;M}A^*_{\lambda_1'\lambda_2;M'}\hat{\rho}_{MM'}, \qquad (3.1)$$

where N is the normalization factor,

$$N=\sum_{\lambda_1,\lambda_2,M,M'}A_{\lambda_1\lambda_2;M}A^*_{\lambda_1\lambda_2;M'}\hat{\rho}_{MM'}, \qquad (3.2)$$

such that $\mathrm{Tr}\rho=1$ and $\hat{\rho}_{MM'}$ is the spin-density matrix of the decaying charmonium state. For an unpolarized state of spin J one simply has

$$\hat{\rho}_{MM'}=\frac{1}{2J+1}\delta_{MM'};$$

however, charmonium states, produced in e^+e^- or $p\bar{p}$ annihilations, have a more interesting spin structure. We shall return to the values of $\hat{\rho}_{MM'}(\chi_{c2})$ in the next section.

The knowledge of the decay amplitudes $A^{\chi_c}_{\lambda_1\lambda_2;M}$ and of the initial-state spin-density matrix $\hat{\rho}(\chi_c)$ allows, via Eqs. (3.1) and (3.2), us to compute the values of $\rho_{\lambda_1\lambda_1'}(M_1)$. These helicity density matrix elements can be measured by observing, in the M_1 meson helicity rest frame [24], the angular distribution of the M_1 decay products.

Supposing that the spin-1 particle M_1 decays into two spinless particles, $M_1\rightarrow AB$ (as it is in the most common case of the $\rho\rightarrow\pi\pi$ decay), one has the normalized angular distribution

$$W(\Theta,\Phi)=\frac{3}{4\pi}[\rho_{0,0}\cos^2\Theta+(\rho_{1,1}-\rho_{1,-1})\sin^2\Theta\cos^2\Phi$$
$$+(\rho_{1,1}+\rho_{1,-1})\sin^2\Theta\sin^2\Phi$$
$$-\sqrt{2}(\mathrm{Re}\rho_{1,0})\sin 2\Theta\cos\Phi], \qquad (3.3)$$

where Θ and Φ are, respectively, the polar and azimuthal angles of the particle A as it emerges from the decay of M_1, in the helicity rest frame of M_1. By integrating Eq. (3.3) over Φ or Θ one can also use

$$W(\Theta)=\tfrac{3}{2}[\rho_{0,0}+(\rho_{1,1}-\rho_{0,0})\sin^2\Theta], \qquad (3.4)$$

$$W(\Phi)=\frac{1}{2\pi}(1-2\rho_{1,-1}+4\rho_{1,-1}\sin^2\Phi). \qquad (3.5)$$

Measurements of the angular distributions of Eqs. (3.3)–(3.5) yield direct information on $\rho_{\lambda_1\lambda_1'}(M_1)$.

IV. $\rho(M_1)$ FOR χ_{c0} AND χ_{c2} DECAYS

A. $\chi_{c0}\rightarrow M_1M_2$

This case, the decay of a spin-zero state, is particularly simple. Eqs. (3.1) and (3.2) read

$$\rho_{\lambda_1\lambda_1'}(M_1)=\frac{1}{N}\sum_{\lambda_2}A^{\chi_{c0}}_{\lambda_1\lambda_2}A^{\chi_{c0}*}_{\lambda_1'\lambda_2}, \qquad (4.1)$$

with

$$N=\sum_{\lambda_1,\lambda_2}|A^{\chi_{c0}}_{\lambda_1\lambda_2}|^2. \qquad (4.2)$$

Recalling Eqs. (2.1)–(2.3) one obtains

$$\rho_{1,1}=\rho_{-1,-1}=\frac{|A^{\chi_{c0}}_{1,1}|^2}{|A^{\chi_{c0}}_{0,0}|^2+2|A^{\chi_{c0}}_{1,1}|^2}, \qquad (4.3)$$

$$\rho_{0,0}=\frac{|A^{\chi_{c0}}_{0,0}|^2}{|A^{\chi_{c0}}_{0,0}|^2+2|A^{\chi_{c0}}_{1,1}|^2}, \qquad (4.4)$$

$$\rho_{\lambda\lambda'}=0,\quad \lambda\neq\lambda', \qquad (4.5)$$

which can be rewritten as

$$\rho_{0,0}=\frac{1}{1+2R_A(\epsilon)}\ , \tag{4.6}$$

$$\rho_{1,1}=\rho_{-1,-1}=\frac{R_A(\epsilon)}{1+2R_A(\epsilon)}\ , \tag{4.7}$$

where

$$R_A(\epsilon)\equiv\frac{|A_{1,1}^{\chi_{c0}}|^2}{|A_{0,0}^{\chi_{c0}}|^2}=4\epsilon^4\left[\frac{f_T}{f_L}\right]^4\left[\frac{I_{1,1}^{\chi_{c0}}(\epsilon)}{I_{0,0}^{\chi_{c0}}(\epsilon)}\right]^2 . \tag{4.8}$$

Equations (4.6)–(4.8) show that, in massless perturbative QCD ($\epsilon=0$), one has $\rho_{00}=1$, $\rho_{11}=0$, as expected. Massive quarks allow (small) nonzero values of ρ_{11}.

B. $\chi_{c2}\to M_1M_2$

This case, the decay of a spin-2 state, is more interesting. The full observed process is typically [25]

$$p\bar{p}\to\chi_{c2}\to M_1M_2\ ,\quad M_1\to AB \tag{4.9}$$

The χ_{c2} produced at rest in $p\bar{p}$ annihilation can never be in a $S_z=\pm2$ state; moreover, if we think of the $p\bar{p}$ annihilation as the annihilation of three massless quark-antiquark pairs [14], then only states with $S_z=\pm1$ are allowed. Nonperturbative effects, like a diquark component of the nucleon, can also lead to χ_{c2} states with $S_z=0$ [26]. In general, the spin-density matrix of the χ_{c2} produced in $p\bar{p}$ (or e^+e^-) annihilations, $\hat{\rho}(\chi_{c2})$, is of the form

$$\begin{aligned}&\hat{\rho}_{2,2}=\hat{\rho}_{-2,-2}=0\ ,\\&\hat{\rho}_{\lambda\lambda'}=0,\quad \lambda\neq\lambda'\ ,\\&\hat{\rho}_{1,1}=\hat{\rho}_{-1,-1}\neq0\ ,\\&\hat{\rho}_{0,0}=1-2\hat{\rho}_{1,1}\neq0\ .\end{aligned} \tag{4.10}$$

In massless perturbative QCD one has the further constraints

$$\begin{aligned}&\hat{\rho}_{1,1}=\hat{\rho}_{-1,-1}=\tfrac{1}{2}\ ,\\&\hat{\rho}_{0,0}=0\ .\end{aligned} \tag{4.11}$$

From Eqs. (2.7)–(2.11), (3.1), (3.2), and (4.10) one obtains, for $\rho_{\lambda\lambda'}(M_1)$,

$$\begin{aligned}\rho_{1,1}=\rho_{-1,-1}=\frac{1}{N}\Bigg[&|\tilde{A}_{1,-1}|^2\left[\frac{1}{2}\hat{\rho}_{1,1}\sin^2\theta(1+\cos^2\theta)+\frac{3}{8}\hat{\rho}_{0,0}\sin^4\theta\right]\\&+|\tilde{A}_{1,0}|^2\left[\frac{1}{2}\hat{\rho}_{1,1}(4\cos^4\theta-3\cos^2\theta+1)+\frac{3}{2}\hat{\rho}_{0,0}\sin^2\theta\cos^2\theta\right]\\&+|\tilde{A}_{1,1}|^2\left[3\hat{\rho}_{1,1}\sin^2\theta\cos^2\theta+\frac{1}{4}\hat{\rho}_{0,0}(3\cos^2\theta-1)^2\right]\Bigg]\ ,\end{aligned} \tag{4.12}$$

$$\begin{aligned}\rho_{1,0}=\rho_{0,1}=-\rho_{-1,0}=-\rho_{0,-1}=\frac{1}{N}|\tilde{A}_{1,0}|\Bigg[&-\frac{1}{2}\left[\frac{3}{2}\right]^{1/2}(|\tilde{A}_{0,0}|-|\tilde{A}_{1,1}|)[2\hat{\rho}_{1,1}\sin\theta\cos\theta(2\cos^2\theta-1)\\&-\hat{\rho}_{0,0}\sin\theta\cos\theta(3\cos^2\theta-1)]\\&+|\tilde{A}_{1,-1}|\left[\hat{\rho}_{1,1}\sin\theta\cos^3\theta+\frac{3}{4}\hat{\rho}_{0,0}\sin^3\theta\cos\theta\right]\Bigg]\ ,\end{aligned} \tag{4.13}$$

$$\begin{aligned}\rho_{1,-1}=\rho_{-1,1}=\frac{1}{N}\Bigg\{&|\tilde{A}_{1,0}|^2\left[-\frac{1}{2}\hat{\rho}_{1,1}(4\cos^4\theta-5\cos^2\theta+1)-\frac{3}{2}\hat{\rho}_{0,0}\sin^2\theta\cos^2\theta\right]\\&+2\,\mathrm{Re}(\tilde{A}_{1,1}\tilde{A}_{1,-1}^*)\left[-\left[\frac{3}{2}\right]^{1/2}\hat{\rho}_{1,1}\sin^2\theta\cos^2\theta+\frac{1}{4}\left[\frac{3}{2}\right]^{1/2}\hat{\rho}_{0,0}\sin^2\theta(3\cos^2\theta-1)\right]\Bigg\}\ ,\end{aligned} \tag{4.14}$$

$$\rho_{0,0}=1-2\rho_{1,1}\ , \tag{4.15}$$

with

$$\begin{aligned}N=&(|\tilde{A}_{0,0}|^2+2|\tilde{A}_{1,1}|^2)[3\hat{\rho}_{1,1}\sin^2\theta\cos^2\theta+\tfrac{1}{4}\hat{\rho}_{0,0}(3\cos^2\theta-1)^2]\\&+|\tilde{A}_{1,-1}|^2[\hat{\rho}_{1,1}\sin^2\theta(1+\cos^2\theta)+\tfrac{3}{4}\hat{\rho}_{0,0}\sin^4\theta]+2|\tilde{A}_{1,0}|^2[\hat{\rho}_{1,1}(4\cos^4\theta-3\cos^2\theta+1)+3\hat{\rho}_{0,0}\sin^2\theta\cos^2\theta]\ .\end{aligned} \tag{4.16}$$

In the massless limit ($\epsilon\to0$) the above results simplify to

$$\rho_{1,1}=\rho_{-1,-1}=\frac{1}{2}\frac{1}{1+3(|\tilde{A}_{0,0}|^2/|\tilde{A}_{1,-1}|^2)[\cos^2\theta/(1+\cos^2\theta)]}\ ,\quad \rho_{0,0}=1-2\rho_{1,1}\ ,\quad \rho_{\lambda\lambda'}=0,\quad \lambda\neq\lambda'\ . \tag{4.17}$$

The same analysis could be readily repeated for the decays of χ_{c2} produced, rather than in the exclusive reaction $p\bar{p}\to\chi_{c2}$ [Eq. (4.9)], in inclusive processes such as $pp\to\chi_{c2}+X$ or $p\bar{p}\to\chi_{c2}+X$. In these cases the spin-density matrix of the produced χ_{c2} is different from that given in Eqs. (4.10) or (4.11); however, it might be estimated by assuming the χ_{c2} production to be dominated by few elementary subprocesses, such as gg fusion. We do not consider this case here.

V. NUMERICAL RESULTS

We are now equipped with the necessary formalism to give numerical estimates of the values of $\rho_{\lambda\lambda'}(M_1)$, the helicity density matrix of a spin-1 particle produced in the decay of a charmonium state, via a process of the type (4.9). We only need to specify the expressions of the distribution amplitudes φ_L and φ_T appearing in Eqs. (2.4), (2.5), and (2.12)–(2.15), and the numerical value of f_L and f_T, the decay constants for longitudinally polarized or transversely polarized vector mesons, respectively [see Eqs. (2.1)–(2.3) and (2.8)–(2.11)]. These quantities shall be taken from the literature [14].

We give here results only for ρ vector mesons ($M_1=\rho^+,\rho^0,\rho^-$), and adopt two different choices of the distribution amplitudes. In one case we follow Chernyak and Zhitnitsky (CZ) [14], who give the following explicit expressions for the distribution amplitudes of ρ mesons:

$$\varphi_L(x)=13.2x(1-x)-36x^2(1-x)^2\ , \tag{5.1}$$

$$\varphi_T(x)=30x^2(1-x)^2\ , \tag{5.2}$$

with

$$f_L\simeq f_T=0.2\ \text{GeV}\ . \tag{5.3}$$

The second choice is the simple symmetric distribution amplitude

$$\varphi_L(x)=\varphi_T(x)=6x(1-x)\ , \tag{5.4}$$

with, again,

$$f_L=f_T=0.2\ \text{GeV}\ . \tag{5.5}$$

The analysis in the case of other final vector mesons ($M_1=K^*$, ϕ, etc.) is obviously similar and is not presented here. Our main goal is that of showing how a measurement of $\rho_{\lambda\lambda'}(M_1)$ and the angular distributions of Eqs. (3.3)–(3.5) could exhibit clear and significant differences between the models with current and constituent quarks. Our results are sensitive to whether we use the same distribution amplitude for longitudinally and transversely polarized vector mesons [$\varphi_L=\varphi_T$, Eq. (5.4)] or different ones [Eqs. (5.1) and (5.2)]. However, assuming $\varphi_L=\varphi_T$, they show almost no dependence on the choice of the distribution amplitudes. Therefore, we limit ourselves to the two cases of Eqs. (5.1)–(5.3) and (5.4) and (5.5).

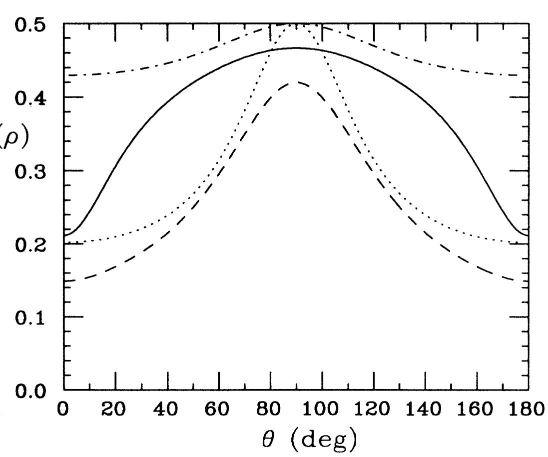

FIG. 2. Values of $\rho_{1,1}(\rho)$ as function of the ρ meson production angle θ. The different curves correspond to the following cases: $m_q\neq 0$ with the symmetric distribution amplitude, Eqs. (5.4) and (5.5) (solid curve); $m_q=0$ with symmetric distribution amplitude (dot-dashed curve); $m_q\neq 0$ with the CZ distribution amplitude, Eqs. (5.1)–(5.3) (dashed curve); $m_q=0$ with the CZ distribution amplitude (dotted curve).

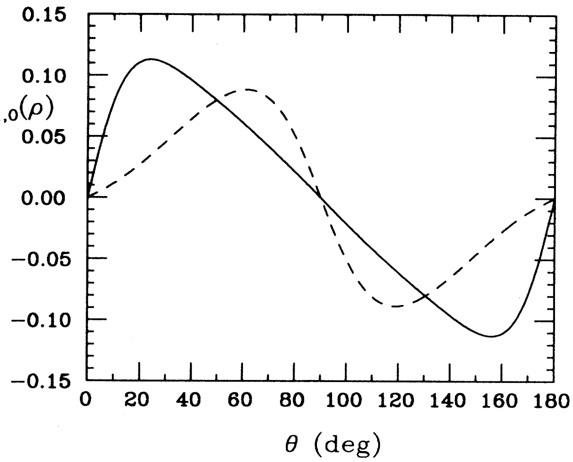

FIG. 3. Values of $\rho_{1,0}(\rho)$ as function of θ; same symbols as in Fig. 2. In case $m_q=0$, one has $\rho_{1,0}=0$.

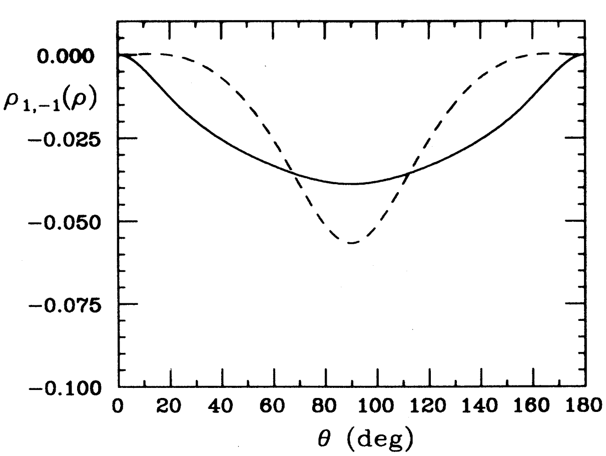

FIG. 4. Values of $\rho_{1,-1}(\rho)$ as function of θ; same symbols as in Fig. 2. In case $m_q=0$, one has $\rho_{1,-1}=0$.

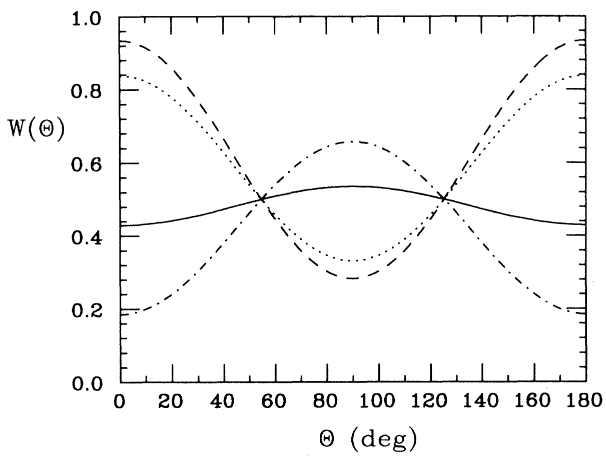

FIG. 5. Plot of the angular distribution, $W(\Theta)$, of the π emitted in the ρ decay. The ρ has been produced at an angle $\theta=30°$. Same symbols as in Fig. 2.

In the case of χ_{c0} decays the only difference between $m_q=0$ and $m_q=xm$ results is the fact that, in the latter case, $\rho_{1,1}(M_1)$ can be different from zero, as it appears from Eqs. (4.7) and (4.8). Its numerical value, however, is almost very tiny and indeed negligible.

χ_{c2} decays are more interesting. Inserting Eqs. (2.8)–(2.15) into Eqs. (4.12)–(4.16), with the help of Eqs. (4.10) and (5.1)–(5.3) or (5.4) and (5.5), one obtains the values of $\rho_{\lambda\lambda'}$ in the constituent quark model ($m_q\neq 0$). The only quantity not yet specified is the value of $\hat{\rho}_{0,0}(\chi_{c2})$, the spin-density matrix of the decaying χ_{c2}; following Ref. [26] we have used $\hat{\rho}_{0,0}(\chi_{c2})\simeq 0.15$, but have explicitly checked that the values of $\rho_{\lambda\lambda'}$ show very little dependence on the values of $\hat{\rho}_{0,0}(\chi_{c2})$ (varied between 0 and 0.2). The analogous results in massless perturbative QCD are obtained as the $\epsilon\to 0$ limit of the previous ones; that is, by inserting Eqs. (2.8)–(2.15) (taken with $\epsilon=0$) into Eqs. (4.17), with the help of Eqs. (4.11) and (5.1)–(5.3) or (5.4) and (5.5).

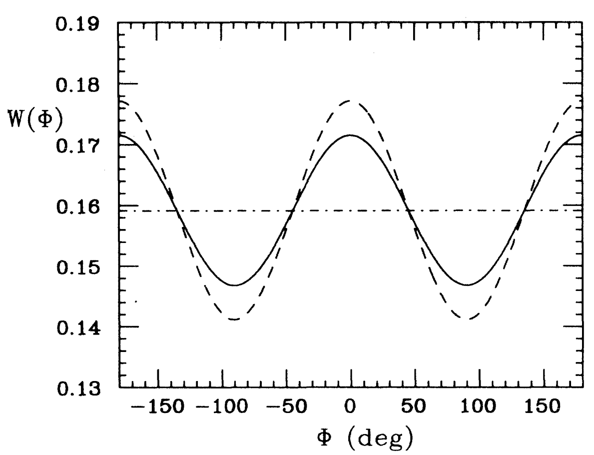

FIG. 6. Plot of the angular distribution, $W(\Phi)$, of the π emitted in the ρ decay. The ρ has been produced at an angle $\theta=90°$. Same symbols as in Fig. 2. In the case of $m_q=0$, one has $W(\Phi)=1/2\pi$.

The results for $\rho_{1,1}(\rho)$, $\rho_{1,0}(\rho)$, and $\rho_{1,-1}(\rho)$ are shown in Figs. 2, 3, and 4, respectively, as a function of θ, the polar angle of the ρ particle in the χ_{c2} rest frame (the polarization of the ρ varies with θ, the angle between the χ_{c2} spin quantization axis and the ρ momentum). The different curves show the results for our two choices of the distribution amplitudes [Eqs. (5.1)–(5.3) or (5.4) and (5.5)], both in the case of massless current quarks and massive constituent quarks. There are clear differences in the different cases; notice that, with massless quarks, one has $\rho_{1,0}=\rho_{1,-1}=0$. We shall comment on the results in the next section.

Different values of $\rho_{\lambda\lambda'}$ lead to different shapes of the angular distributions of the π produced in the ρ decay ($\rho\to\pi\pi$, in the ρ helicity rest frame), Eqs. (3.3)–(3.5). This can be seen in Figs. 5 and 6, which show $W(\Theta)$ and $W(\Phi)$ with massive and massless quarks for our two choices of distribution amplitudes and for ρ mesons produced, respectively, at $\theta=30°$ and 90°. Similar results hold for different production angles.

VI. COMMENTS AND CONCLUSIONS

We have studied the polarization of ρ mesons produced in the decays of χ_{c0} and polarized χ_{c2} states. As usual with spin physics, the measurement of some elements of the helicity density matrix of the ρ mesons, although difficult, could allow severe tests of different models and schemes. Such measurements might be available in the near future from experiments in progress at Fermilab.

Following a previous paper [10] we have studied mass corrections to the usual asymptotic perturbative QCD scheme. Some of our results are shown in Figs. 2–6 for χ_{c2} decays. The matrix elements $\rho_{1,1}(\rho)$ (Fig. 2) and $\rho_{0,0}=1-2\rho_{1,1}$ are the only ones which can be different from zero in massless perturbative QCD. Even for them, the actual numerical values are sizably different from case to case. For example, $\rho_{1,1}(\rho)$, as given by massless perturbative QCD with the CZ distribution amplitude [Eqs. (5.1)–(5.3)] (dotted curve in Fig. 2), differs significantly from the constituent quark result with the intuitive symmetric distribution amplitude, Eqs. (5.4) and (5.5) (solid curve in Fig. 2). Notice that, in principle, a precise measurement of $\rho_{1,1}$ could also discriminate, independently of whether we consider massless or massive quarks, between distribution amplitudes with $\varphi_L=\varphi_T$ or $\varphi_L\neq\varphi_T$.

The matrix elements $\rho_{1,0}$ and $\rho_{1,-1}$ are zero in massless perturbative QCD; they *are not* zero with constituents quarks and their measurement would be a definitive support in favor of mass corrections, independently of the choice of the distribution amplitudes. In particular, $\rho_{1,0}$ is sizable, with a typical θ dependence; its measurement, however, requires the study of the full angular distribution, Eq. (3.3), of difficult measurement. $\rho_{1,-1}$, which appears in $W(\Phi)$, might also be problematic to detect, due to its tiny value.

In Figs. 5 and 6 we show the angular distributions of the π produced in the decay of the polarized $\rho,\rho\to\pi\pi$, according to Eqs. (3.4) and (3.5); this is the quantity which is actually observed. Again, an accurate study of $W(\Theta)$, which depends on $\rho_{1,1}$, should allow to discriminate among the different cases. $W(\Phi)$ is constant $[W(\Phi)=1/2\pi]$ when $\rho_{1,-1}=0$, that is, in massless perturbative QCD; instead, it shows typical oscillations in case of constituent quarks, hopefully large enough to be detected. Let us stress once more that such result originates entirely from assuming $m_q\neq 0$; whereas the actual values of the diagonal helicity density matrix elements depend both on the quark masses and (to some extent) on the choice of the distribution amplitudes, nonzero values of the off-diagonal matrix elements can only be generated by massive quarks.

As we repeatedly stressed, charmonium decays are still affected by many nonperturbative and higher-order contributions which may not yet be negligible in the Q^2 region involved. However, the processes and the measurements considered here should mainly be sensitive to mass effects, with the only possible exception of intrinsic $k_\perp$ effects, which have never been investigated. Detailed studies of these mass effects, even though through difficult spin measurements, would certainly help in formulating useful quantitative models to deal with nonperturbative QCD phenomena.

---

[1] S. J. Brodsky and G. P. Lepage, Phys. Rev. D **24**, 2848 (1981).

[2] V. L. Chernyak and A. R. Zhitnitsky, Nucl. Phys. **B201**, 492 (1982).

[3] A. Andrikopolou, Z. Phys. C **22**, 63 (1984).

[4] V. L. Chernyak and I. R. Zhitnitsky, Nucl. Phys. **B246**, 52 (1984).

[5] P. H. Damgaard, K. Tsokos, and E. Berger, Nucl. Phys. **B259**, 285 (1985).

[6] V. L. Chernyak, A. A. Ogloblin, and I. R. Zhitnitsky, Z. Phys. C **42**, 569 (1989); **42**, 583 (1989).

[7] N. G. Stefanis and M. Bergmann, this issue, Phys. Rev. D **47**, R3685 (1993).

[8] S. J. Brodsky, G. P. Lepage, and S. F. Tuan, Phys. Rev. Lett. **59**, 621 (1987).

[9] M. Anselmino, F. Caruso, and F. Murgia, Phys. Rev. D **42**, 3218 (1990).

[10] M. Anselmino, R. Cancelliere, and F. Murgia, Phys. Rev. D **46**, 5049 (1992).

[11] A. Duncan and A. H. Mueller, Phys. Lett. **93B**, 119 (1980).

[12] G. P. Lepage and S. J. Brodsky, Phys. Rev. D **22**, 2157 (1980); S. J. Brodsky and G. P. Lepage, in *Perturbative Quantum Chromodynamics,* edited by A. H. Mueller (World Scientific, Singapore, 1989).

[13] A. H. Mueller, Phys. Rep. **73**, 237 (1981).

[14] V. L. Chernyak and A. R. Zhitnitsky, Phys. Rep. **112**, 173 (1984).

[15] M. Anselmino, F. Caruso, and F. Murgia, in Proceedings of the Adriatico Research Conference on Polarization Dynamics in Nuclear and Particle Physics, Trieste, Italy, 1992 (unpublished).

[16] M. Anselmino, F. Caruso, and S. Forte, Phys. Rev. D **44**, 1438 (1991).

[17] M. Anselmino, F. Caruso, S. Joffily, and J. Soares, Mod. Phys. Lett. A **6**, 1415 (1991).

[18] M. Anselmino and F. Murgia, Z. Phys. C (to be published).

[19] M. Benayoun, V. L. Chernyak, and I. R. Zhitnitsky, Nucl. Phys. **B348**, 327 (1991).

[20] M. Anselmino, M. Genovese, and E. Predazzi, Phys. Rev. D **44**, 1597 (1991).

[21] S. Weinberg, Phys. Rev. Lett. **65**, 1181 (1990).

[22] R. Barbieri, R. Gatto, and R. Kögerler, Phys. Lett. **60B**, 183 (1976).

[23] F. Murgia, Doctorate thesis, University of Torino (1992).

[24] See, e.g., C. Bourrely, J. Soffer, and E. Leader, Phys. Rep. **59**, 95 (1980).

[25] T. A. Armstrong *et al.*, Nucl. Phys. **B373**, 35 (1992).

[26] M. Anselmino, F. Caruso, and R. Mussa, Phys. Rev. D **45**, 4340 (1992).